# Irradiation-induced oxygen knock-out and its role in bismuth cuprate superconductors

S. K. Bandyopadhyay, P. Barat, and Pintu Sen
*Variable Energy Cyclotron Centre, 1/AF, Bidhan Nagar, Calcutta-700 064, India*

A. K. Ghosh and A. N. Basu
*C.M.P.R.C., Department of Physics, Jadavpur University, Calcutta-700 032, India*

B. Ghosh
*Saha Institute of Nuclear Physics, 1/AF, Bidhan Nagar, Calcutta-700 064, India*
(Received 20 January 1998; revised manuscript received 20 April 1998)

Charged particle irradiations have been carried out on Bi-2212 and Pb-doped Bi-2223 with 40-MeV $\alpha$ particles and 15-MeV protons. The purpose was to investigate the knock-out of oxygen caused by particle irradiation and its effects on superconductivity. Studies with respect to x-ray diffraction patterns, $T_c$, resistivity, oxygen contents, etc., have been undertaken on samples, unirradiated as well as irradiated at various doses for comparison. A remarkable difference has been observed between Bi-2212 and Bi-2223 with respect to the irradiation-induced knock-out of oxygen. In Bi-2212, the oxygen knock-out plays a dominant role and there is an increase in $T_c$ by particle irradiation for the sample overdoped with oxygen. On the other hand, in Bi-2223, there has been a decrease in $T_c$ except for protons at a low dose and the knock-out of oxygen is not significant. There has been an increase in resistivity in general by irradiation. At a high dose of $1\times10^{16}\alpha/\mathrm{cm}^2$, there is a change to nonmetallic behavior in resistivity with three-dimensional variable range hopping conductivity in both Bi-2212 and Bi-2223. [S0163-1829(98)09338-2]

## I. INTRODUCTION

Physical properties of superconducting materials are strongly affected by structural defects and disorder.[1] Particle irradiation is often used to produce intrinsic damage in a controlled manner to study the influence of defects and disorder on the superconducting properties in a wide range of damage concentrations. In the case of superconductors, it is the nonionizing energy loss (NIEL) causing displacement of atoms that plays a significant role in controlling physical properties like critical temperature, resistivity, critical current density, etc. The NIEL is measured by displacement per atom or d.p.a. For a particular irradiation, d.p.a. is proportional to the fluence or dose of irradiation.

In conventional superconductors, point defects generated by radiation-induced atomic displacements change density of states around the Fermi surface, causing thereby depression of $T_c$. The change in $T_c$ as a function of the radiation-induced increase of the residual resistivity at zero temperature ($\Delta\rho_0$) reveals in general a universal behavior depending on the electronic density of states (DOS) around the Fermi level $E_F$.[2] There are some instances of increase in $T_c$ as in $Mo_3Si$ and $Nb_3Ir$.[1]

In the case of high-$T_c$ superconductors also, it has been seen that atomic displacements caused by NIEL of incident particles control the change of $T_c$ and other physical properties as a function of fluence.[1] Light charged particles in moderate energy ranges generate mostly point defects and line defects, dislocations, etc. However, here the effect of irradiation is complex. The high-$T_c$ cuprate superconductors are nonstoichiometric, particularly with respect to oxygen and irradiation-induced knock-out and disordering of oxygen plays a crucial role in controlling various parameters such as $T_c$, resistivity, etc. The high-$T_c$ oxide superconductors have a rather low DOS at $E_F$ compared to their low-$T_c$ counterparts and by lowering the oxygen concentration, $N(E_F)$ can be reduced further.[3]

We had earlier observed an increase in $T_c$ by 20-MeV $\alpha$ irradiation on one side of polycrystalline $Bi_2Sr_2CaCu_2O_{8+x}$ (Bi-2212) samples of $T_c$ 65 K.[4] The increase in $T_c$ was monotonic with dose and the $T_c$ change was presumed to be due to knock-out of oxygen by $\alpha$ particles from the unirradiated sample with much excess oxygen (overdoped). Irradiation was carried on one surface of the sample. The range of 20-MeV $\alpha$ in Bi-2212 is quite small ($\sim$100 $\mu$m). So, in the sample of around 1 mm thickness (as used in earlier irradiation experiments), the damage did not propagate to much depth. Hence, bulk damage and change in oxygen content could not be ascertained, as the radiation-induced oxygen knock-out could not occur in the bulk. To investigate the bulk damage, we have adopted the following modifications: (1) The thickness of the sample has been reduced from 1 mm to 0.5 mm. (2) The energy of $\alpha$ has been increased from 20 MeV to 40 MeV to have longer range and hence larger depth of damage. (3) Irradiation has been carried out on both surfaces of the sample to obtain fairly uniform bulk damage.

In this paper, we report systematic investigations of the effects of 40-MeV $\alpha$-particle and 15-MeV proton irradiations on bulk polycrystalline samples of Bi-2212 and Bi-2223 and 40-MeV $\alpha$ irradiation on Bi-2212 single crystals with respect to $T_c$, resistivity, oxygen knock-out, structural change, etc. The motivation for undertaking the experiments on bulk samples was to study the irradiation-induced knock-out of oxygen through bulk measurements like iodometric estimation of oxygen which can be carried out only in bulk polycrystalline samples.

 

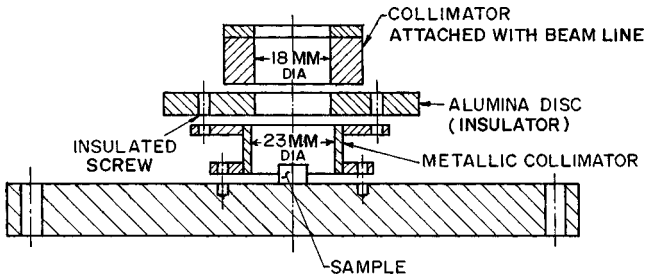


FIG. 1. Target holder assembly for irradiation.

The primary factor for radiation damage studies is displacement per atom or d.p.a. Using the TRIM-95 version of the Monte Carlo simulation code TRIM developed by Biersack and Haggmark,[5] we have calculated the d.p.a.'s of various ions in Bi-2212 and Bi-2223. Considering the average displacement energy of atoms to be $\approx$20 eV, d.p.a.'s at a dose of $1\times10^{15}$ particles/cm$^2$ for 40-MeV $\alpha$ and 15-MeV protons are $1.86\times10^{-4}$ and $1.26\times10^{-5}$, respectively, in polycrystalline Bi-2212 of 0.5 mm thickness. The corresponding values in polycrystalline Bi-2223 of 0.5 mm thickness are $1.9\times10^{-4}$ and $1.27\times10^{-5}$, respectively. Doses were employed aiming at appreciable change in physical properties without causing a major structural breakdown or amorphization. Hence, we have limited the irradiation dose up to the order of $10^{16}\alpha$/cm$^2$ corresponding to a d.p.a. of the order $10^{-3}$.

## II. EXPERIMENTAL DETAILS

Polycrystalline samples of Bi-2212 and Bi-2223 with nominal compositions $Bi_2Sr_2CaCu_2O_{8+x}$ and $Bi_{1.84}Pb_{0.34}Sr_{1.91}Ca_{2.03}Cu_{3.06}O_{10+x}$, respectively, were prepared by a typical solid-state reaction[6,7] starting from nitrates of the respective metals. The Bi-2212 single crystal was obtained by the alkali flux method from polycrystalline Bi-2212 using equimolar mixtures of KCl and NaCl as fluxes.

The samples for irradiation were mounted in a target holder assembly which is schematically shown in Fig. 1. It consists of an aluminum flange over which the samples were mounted. Aluminum was employed as flange material since the nuclear reaction cross section of 40-MeV $\alpha$ particles and 15-MeV protons with aluminum is very low. The dose accumulating on the target material (sample) kept on the flange was estimated from the total charge of projectile particles ($\alpha$ or proton) deposited on the samples which was measured with the help of a Danfys current integrator and scalar electrically connected to the flange. The target flange was insulated from the beam tube by a perspex flange and teflon bush in the screws connecting the target flange and the beam line. A defocused beam of projectile particles was taken to obtain uniform distribution of irradiation dose on the target. We employed pressurized water (24 psig) flowing through the target flange which yielded a temperature rise of $\sim$10 °C of the sample as monitored by a thermocouple sensor placed inside a groove of the flange in close proximity of the sample. This temperature rise did not affect the radiation-induced defects in any significant way.

Polycrystalline Bi-2212 samples of $T_c=73$ K in the form of pellets of thickness 0.5 mm were irradiated with 40-MeV $\alpha$ particles with doses of $2\times10^{15}$, $4\times10^{15}$, $6\times10^{15}$, $8\times10^{15}$, and $1\times10^{16}\alpha$/cm$^2$. For proton irradiation, the doses employed were $5\times10^{13}$, $1\times10^{14}$, $1\times10^{15}$, $2\times10^{15}$, and $5\times10^{15}$ protons/cm$^2$. We also carried out studies on single crystals free from effects of granularity of polycrystals. Bi-2212 single crystals of $\sim$35 $\mu$m thickness and $T_c=81$ K were irradiated with 40-MeV $\alpha$ particles at doses of $2\times10^{14}$ and $2\times10^{15}\alpha$/cm$^2$. The polycrystalline Bi-2223 samples were irradiated with $1\times10^{15}$, $2\times10^{15}$, $3\times10^{15}$, $4\times10^{15}$, $1\times10^{16}$, and $1.5\times10^{16}\alpha$/cm$^2$. The unirradiated sample was of $T_c$ 112 K and room-temperature resistivity ($\rho_{300}$) 3.1 m$\Omega$ cm. The doses employed for protons in polycrystalline Bi-2223 were $5\times10^{13}$, $1\times10^{14}$, $1\times10^{15}$, $2\times10^{15}$, $5\times10^{15}$, $8\times10^{15}$, and $1\times10^{16}$ protons/cm$^2$. The unirradiated sample was of $T_c$ 103.6 K and $\rho_{300}$ of 3.65 m$\Omega$ cm. All the irradiations were carried out at ambient rather than at low temperature, as the post-irradiation measurements were done at room temperature. This would eliminate annealing at room temperature of defects generated during irradiation. For each dose, a few number of samples were earmarked.

All samples were characterized by powder x-ray diffraction patterns by Phillips Diffractometer PW1710 using Cu-K$\alpha$ radiation of wavelength around 1.54 Å. Resistivities of the unirradiated as well as the irradiated samples were measured by a four-probe technique using a Keithley 182 digital nanovoltmeter with resolution of 1 nV and a Lake Shore 120 constant current source. Current leads were attached by the conducting paints covering the thickness sides of the samples so that the resistivity measured by the voltage drop across voltage leads reflected the bulk one. The current through the samples was typically 1 mA.

The oxygen in excess of the stoichiometry was quantitatively assayed by iodometry, which in principle is essentially the volumetric estimation of the iodine liberated by oxidation of iodide by the excess oxygen. The quantity of iodine proportional to the excess oxygen is titrated with sodium thiosulphate solution using starch indicator. But, the presence of CuI affects the end point of titration in the way that iodine is liberated partially. We eliminated this by complexing Cu(II) with citrate, which prevents reduction of Cu(II) to Cu(I).[8] The sample in powder form was dissolved in a minimum amount of ice cold HBr. The solution was prepared in a conical flask closed with a teflon stopper and kept in ice to prevent the escape of bromine by evaporation. Dissolution of the sample was enhanced by stirring. Five milliliters of 1 molar sodium citrate was added to the solution. Potassium iodide was added to it and the mixture well stirred and kept in the dark. It was titrated with sodium thiosulphate with constant stirring. Excess oxygen content thus estimated volumetrically was precise and accurate to $\pm0.001$.

## III. RESULTS AND DISCUSSIONS

### A. X-ray studies

X-ray diffraction patterns of some irradiated Bi-2212 and Bi-2223 samples are presented in Figs. 2 and 3, respectively. Figures 2(a)–2(f) give patterns for Bi-2212 polycrystalline samples, unirradiated as well as irradiated with 40-MeV $\alpha$ particles at various doses. The characteristic reflection lines of the unirradiated samples are present in the irradiated

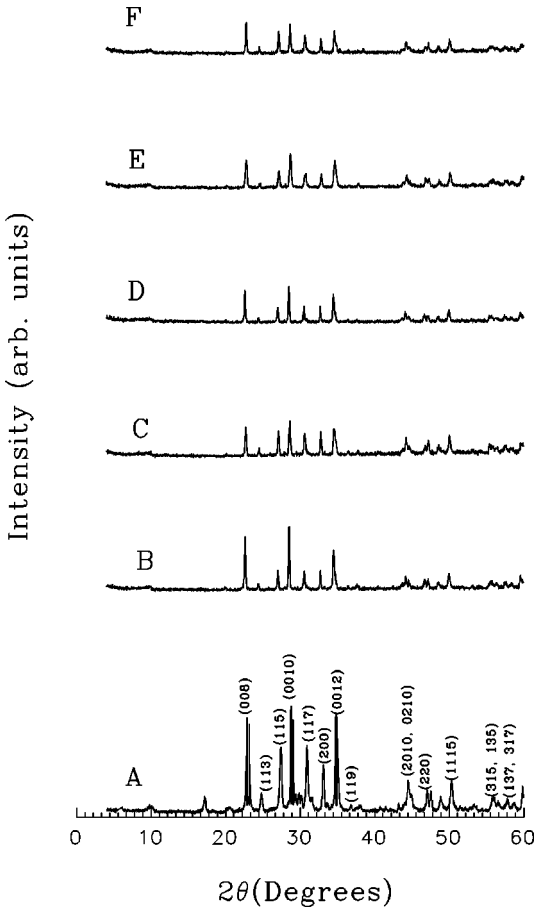


FIG. 2. XRD patterns of polycrystalline Bi-2212 at various doses. A: zero dose (unirradiated); B: $2\times10^{15}\alpha/\mathrm{cm}^2$; C: $4\times10^{15}\alpha/\mathrm{cm}^2$; D: $6\times10^{15}\alpha/\mathrm{cm}^2$; E: $8\times10^{15}\alpha/\mathrm{cm}^2$; F: $1\times10^{16}\alpha/\mathrm{cm}^2$.

samples. Figure 3 depicts the x-ray diffraction (XRD) patterns for the unirradiated Bi-2223 sample as compared to some representative 40-MeV $\alpha$-irradiated samples at doses of $1\times10^{14}$, $1\times10^{15}$, and $2\times10^{14}$ $\alpha/\mathrm{cm}^2$. Here also, the characteristic reflection lines of the unirradiated sample are retained in irradiated samples. Similar characteristics in x-ray diffraction patterns are noticed in proton-irradiated samples of Bi-2212 and Bi-2223.

There have been slight shifts of 00l peaks in $\alpha$-irradiated Bi-2212 samples towards lower angles as compared to those of the unirradiated sample. The average lattice *c*-parameters obtained from indexing various 00l peaks are presented in Table I. We have observed an overall increase in the *c* parameter in the irradiated Bi-2212 samples. The overall increase in the *c* parameter accompanied with the decrease in oxygen content due to particle irradiation was also observed in $YBa_2Cu_3O_{7-\delta}$ (YBCO) and Bi-2212 by Linker *et al.*[9] In the case of Bi-2212 irradiated with 40-MeV $\alpha$ too, the increase in the *c* parameter can be explained by the irradiation-induced knock-out of oxygen, whereby the hole carrier concentration in the $CuO_2$ plane decreases, causing increases in both *a* and *c* parameters.

The retention of distinct reflection lines in all irradiated samples clearly indicates that there has not been any transition from crystalline to amorphous phase due to irradiation. The slight broadening of lines can be explained by the fact

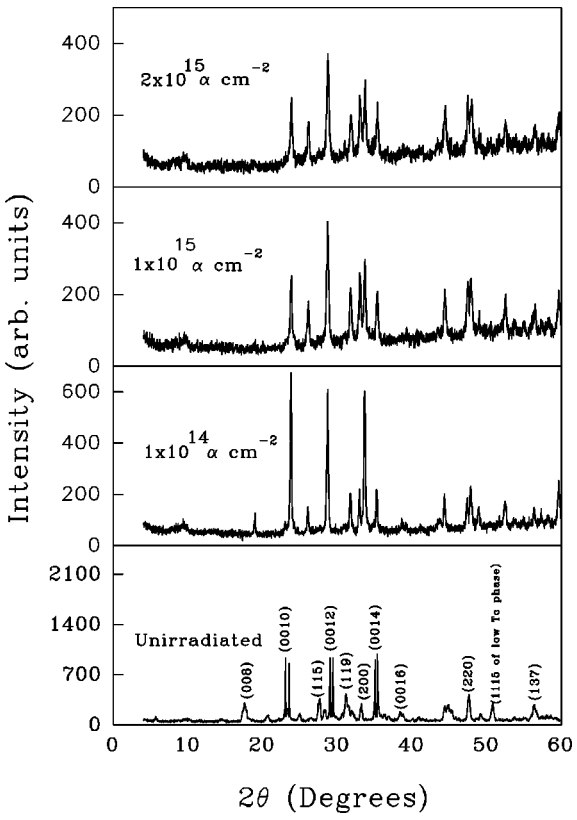


FIG. 3. XRD patterns of unirradiated and $\alpha$-irradiated Bi-2223.

that at low d.p.a., the grain boundaries being regions of highest energy have been subjected to disorder caused by particle irradiation. The point-defect density in the early stage of irradiation is higher near a grain boundary than in the bulk of the grain.[10,11] The retainment of characteristic reflection lines of x-rays in our case bears signature to the fact that there has not been any phase transition, which was earlier observed in the case of Bi-2212 thin films irradiated with 50-KeV $\alpha$ particles.[12]

### B. $T_c$ and resistivity

Resistivity versus temperature plots of some irradiated samples of 40-MeV $\alpha$-irradiated Bi-2212 polycrystals and single crystals as compared to the unirradiated samples are presented in Figs. 4(a), 4(b), and 5, respectively. Figures 6(a) and 6(b) give resistivity versus temperature plots for the polycrystalline Bi-2223 samples, unirradiated and irradiated at doses of $1\times10^{15}$, $2\times10^{15}$, $3\times10^{15}$, $4\times10^{15}$, and 1

TABLE I. Change of lattice parameter of polycrystalline Bi-2212 with dose.

| Dose ($\alpha/\mathrm{cm}^2$) | | Average *c* Parameter (Å) |
|---|---|---|
| 0 | (A) | 30.801 |
| $2\times10^{15}$ | (B) | 31.303 |
| $4\times10^{15}$ | (C) | 31.223 |
| $6\times10^{15}$ | (D) | 31.341 |
| $8\times10^{15}$ | (E) | 31.125 |
| $1\times10^{16}$ | (F) | 31.223 |

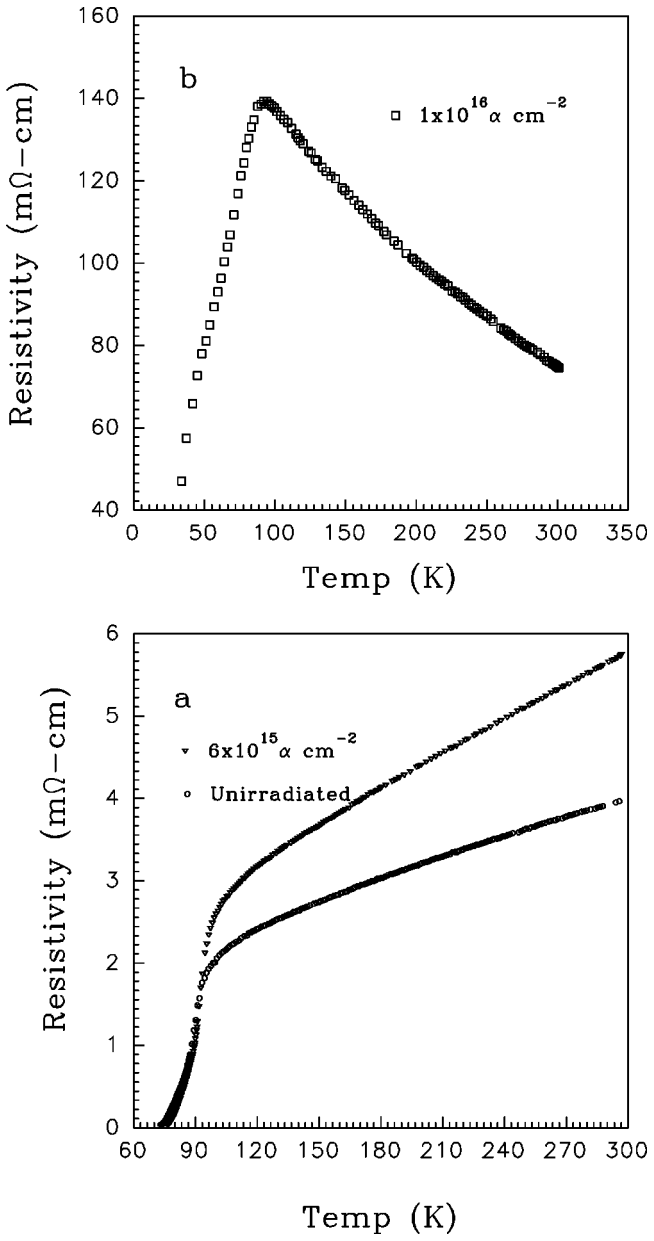


FIG. 4. (a) Resistivities of unirradiated and irradiated polycrystalline Bi-2212. (b) Resistivity of polycrystalline Bi-2212 at highest dose.

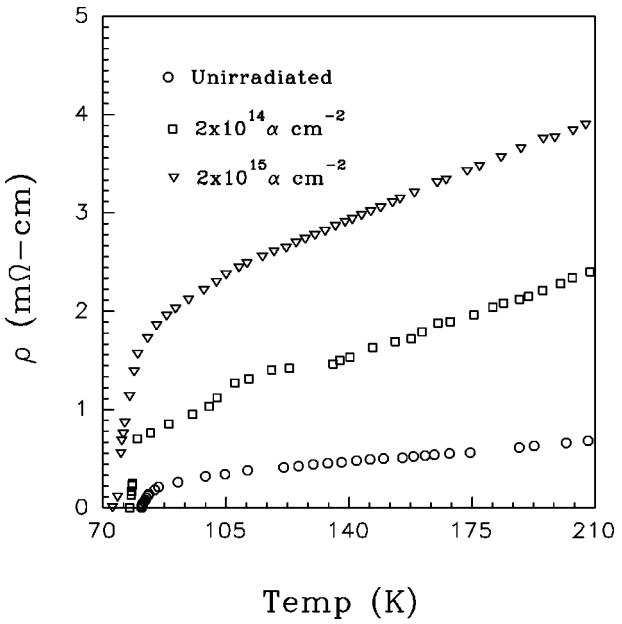


FIG. 5. Resistivities of Bi-2212 single crystals, unirradiated and irradiated at various doses.

$\times 10^{16}\alpha/\mathrm{cm}^2$. $T_c$ $(R=0)$ and the oxygen content $(x)$ in excess of the stoichiometric values of $\alpha$-irradiated Bi-2212 and Bi-2223 polycrystalline samples are presented in Table II. Table III lists $T_c(R=0)$ and excess oxygen contents $(x)$ of proton irradiated polycrystalline Bi-2212 and Bi-2223 samples at different doses. $T_c(R=0)$ of the unirradiated Bi-2212 polycrystalline sample was 73.1 K. There has been an increase in $T_c$ up to the dose of $6\times 10^{15}\alpha/\mathrm{cm}^2$. The sample irradiated at the highest dose of $1\times 10^{16}\alpha/\mathrm{cm}^2$ showed nonmetallic behavior in resistivity from 300 to 100 K and in the case of Bi-2212, there was a fall in resistivity around 100 K but $T_c(R=0)$ was $<10$ K, the lowest temperature achievable in our cryogenerator. From Table II, we see that oxygen contents of Bi-2212 samples have decreased with dose. In the case of proton irradiation too, there is marginal knock-out of excess oxygen as evident from Table III. Below the dose of $1\times 10^{15}$ protons/cm$^2$, the knock-out is not appreciable and the change in $T_c$ is not significant. Figure 7 shows the trends of $T_c(R=0)$ and excess oxygen content versus dose in $\alpha$-irradiated Bi-2212. Unlike polycrystalline Bi-2212, there has been no increase in $T_c$(onset) and no change in oxygen content in particle irradiated Bi-2223. In most cases (both proton and $\alpha$ irradiation on Bi-2212 and Bi-2223), there are increases of transition widths $(\Delta T_c)$ as evident from Figs. 4–6.

The unirradiated polycrystalline Bi-2212 of $T_c=73$ K has an $x$ value (i.e., oxygen content in excess to that of stoichiometry) of 0.204 as evident from iodometric estimations. Excess oxygen is the source of the hole carrier in these cuprates. $T_c$ is related to the hole carrier density and hence excess oxygen content $(x)$. In Bi-2212, $T_c$ increases initially with $x$, goes to a maximum, and then decreases with the increase of $x$ following a typical dome shaped curve.[13,14] The excess oxygen contents corresponding to the peak values of $T_c$ vary from 0.15 to 0.16.[13,14] The excess oxygen in unirradiated polycrystalline Bi-2212 (0.204) corresponded to the right or the overdoped side of the $T_c$ versus oxygen dome-shaped curve in Fig. 3a of Ref. 13. As oxygen content of the unirradiated sample was in excess to that ($\approx 0.16$) corresponding to the maximum $T_c$, it is expected that there would be an increase in $T_c$ on reduction of oxygen content. Thus, the increase in $T_c$ for the irradiated samples was due to the loss of excess oxygen. The peak of $T_c(R=0)$ corresponds to a dose of $\approx 6\times 10^{15}\alpha/\mathrm{cm}^2$ and the equivalent oxygen content is 0.10 as revealed from Fig. 7. For a comparative study, we have plotted normalized $T_c$'s $[T_c/T_c(\mathrm{max})$, where $T_c(\mathrm{max})$ is the maximum $T_c$ attained for the system] versus excess oxygen content. Figure 8 shows such plots for both normalized $T_c(R=0)$ and $T_c$(onset) of 40-MeV $\alpha$-irradiated Bi-2212 along with normalized $T_c$ of Allgeier and Schilling.[13] Normalized $T_c$(onset) peaking at $x\approx 0.15$ in our case behaves similar to their case.

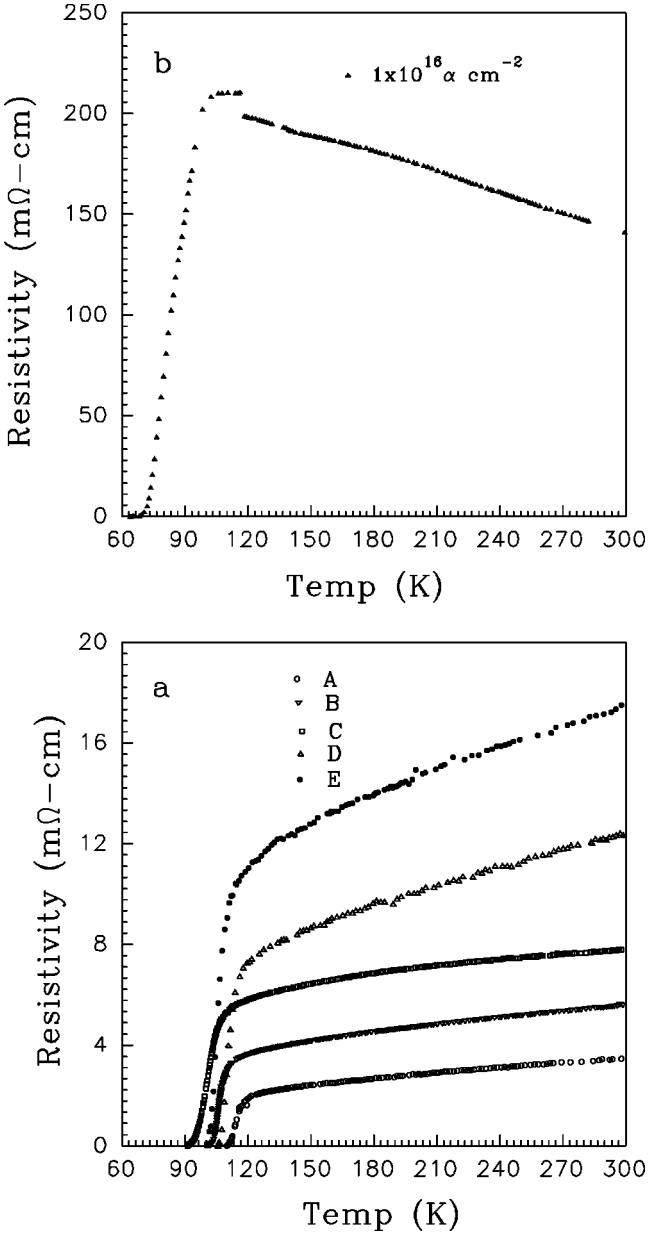


FIG. 6. (a) Resistivity plots of $\alpha$-irradiated Bi-2223. A: unirradiated; B: $1\times10^{15}\alpha/\mathrm{cm}^2$ ; C: $2\times10^{15}\alpha/\mathrm{cm}^2$ ; D: $3\times10^{15}\alpha/\mathrm{cm}^2$; E: $4\times10^{15}\alpha/\mathrm{cm}^2$. (b) Resistivity of Bi-2223 irradiated with $\alpha$-particles at high doses.

$T_c$(onset) values in case of proton irradiation are slightly different than in case of $\alpha$ irradiation, even when excess oxygen contents are the same. Actually, the changes of $T_c$(onset) with excess oxygen in different cases are qualitatively similar, not quantitatively and hence the peaking of $T_c$(onset) also varies in different cases.[13,14] Thus, there is not exactly one to one correspondence between $T_c$(onset) and oxygen content for different systems. $T_c$ depends on carrier concentration, which is controlled by oxygen and other ions. In these nonstoichiometric defect based superconductors, cationic vacancies and other defects also control carrier concentration. Irradiation-induced defects and disorder manifest in not only oxygen displacements, but also in other cationic displacements (such as Cu, Sr, etc.). The extents of these are also different in $\alpha$ and proton irradiation. The cumulative effects of all these may give rise to different values of $T_c$(onset) for $\alpha$ and proton irradiation, even when the oxygen contents are the same.

TABLE II. Variation of $T_c$, excess oxygen, and other parameters with dose for polycrystalline Bi-2212 and Bi-2223 irradiated with 40-MeV $\alpha$ particles.

| Dose ($\alpha/\mathrm{cm}^2$) | $T_c(R=0)$ (K) | $T_c$(onset) (K) | Excess oxygen ($x$) |
|---|---|---|---|
| | | Bi-2212 | |
| 0 | 73.1 | 90.5 | 0.204 |
| $2\times10^{15}$ | 74.3 | 92.3 | 0.190 |
| $4\times10^{15}$ | 75.8 | 94.8 | 0.150 |
| $6\times10^{15}$ | 76.3 | 92.7 | 0.100 |
| $8\times10^{15}$ | 66.5 | 88.5 | 0.080 |
| $1\times10^{16}$ | | $T_c$(onset) around 100 K | |
| | | Bi-2223 | |
| 0 | 112.0 | 122.0 | 0.100 |
| $1\times10^{15}$ | 111.0 | 122.0 | 0.100 |
| $2\times10^{15}$ | 108.0 | 122.0 | 0.100 |
| $3\times10^{15}$ | 105.8 | 121.8 | 0.100 |
| $4\times10^{15}$ | 103.6 | 121.6 | 0.096 |
| $1\times10^{15}$ | 64.0 | 94.0 | 0.096 |

$T_c$(onset) is the temperature at which grains become superconducting. The granular $T_c$ is controlled by the lattice oxygen content. Hence, $T_c$(onset) is affected by $x$, the excess oxygen, whereas $T_c(R=0)$ is controlled by the intergranular links too. As discussed earlier, in polycrystalline samples, grain boundaries are regions of the highest energy and most vulnerable for radiation damage such as enhanced formation of defects, outdiffusion of oxygen, etc., which lead to destruction of weak intergranular links[1] and depression of $T_c(R=0)$ even at lower doses of irradiation, whereas the granular $T_c$, i.e., $T_c$(onset) is not affected.

TABLE III. $T_c$ and oxygen content of proton irradiated Bi-2212 and Bi-2223 samples.

| Dose (protons/$\mathrm{cm}^2$) | $T_c(R=0)$ (K) | $T_c$(onset) (K) | Excess oxygen ($x$) |
|---|---|---|---|
| | | Bi-2212 | |
| 0 | 73.1 | 90.5 | 0.204 |
| $5\times10^{13}$ | 73.5 | 91.5 | 0.204 |
| $1\times10^{14}$ | 73.5 | 92.5 | 0.203 |
| $1\times10^{15}$ | 74.0 | 94.0 | 0.200 |
| $2\times10^{15}$ | 74.8 | 95.8 | 0.195 |
| $5\times10^{15}$ | 73.9 | 95.9 | 0.180 |
| | | Bi-2223 | |
| 0 | 103.6 | 120.6 | 0.100 |
| $5\times10^{13}$ | 104.5 | 120.5 | 0.100 |
| $1\times10^{14}$ | 103.5 | 120.5 | 0.100 |
| $1\times10^{15}$ | 103.2 | 120.7 | 0.100 |
| $2\times10^{15}$ | 103.0 | 120.5 | 0.100 |
| $5\times10^{15}$ | 103.0 | 120.5 | 0.100 |
| $8\times10^{15}$ | 100.0 | 119.0 | 0.095 |
| $1\times10^{16}$ | 96.0 | 118.0 | 0.095 |

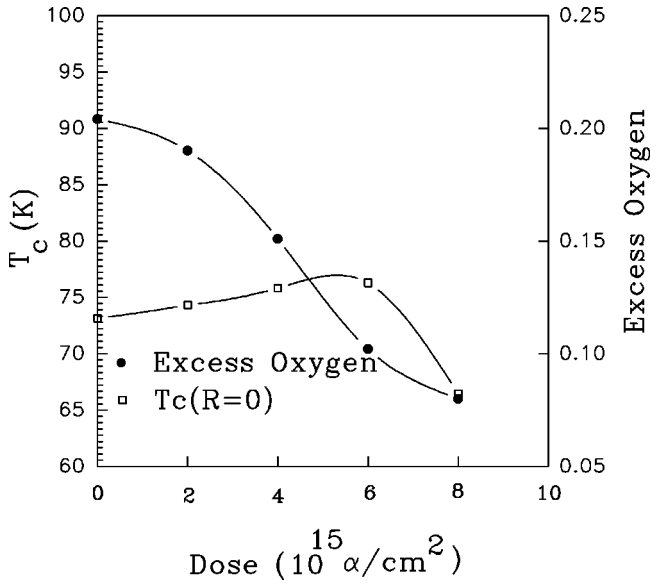


FIG. 7. Change of $T_c$ and oxygen content with dose for polycrystalline Bi-2212.

It is the radiation-induced destruction of weak intergranular links in polycrystalline samples that causes an increase in the transition width and fast decrease in $T_c(R=0)$ of the 40-MeV $\alpha$-irradiated Bi-2212 sample at higher dose where it is underdoped with respect to oxygen (Fig. 8). This is reflected in the overdoped region too. In the overdoped region, the irradiation-induced knock-out of oxygen increases $T_c$ on the one hand and the destruction of intergranular links causes a decrease in $T_c$. Hence, the $T_c(R=0)$ versus excess oxygen curve is less sharp than that of Allgeier and Schilling as reflected in Fig. 8.

In the case of the unirradiated single crystal (as grown), $T_c$ increased to 83 K after annealing in oxygen. Thus, it was in the underdoped region of the dome shaped curve.[13] So, a decrease in $T_c$ by 40-MeV $\alpha$ irradiation can be explained by

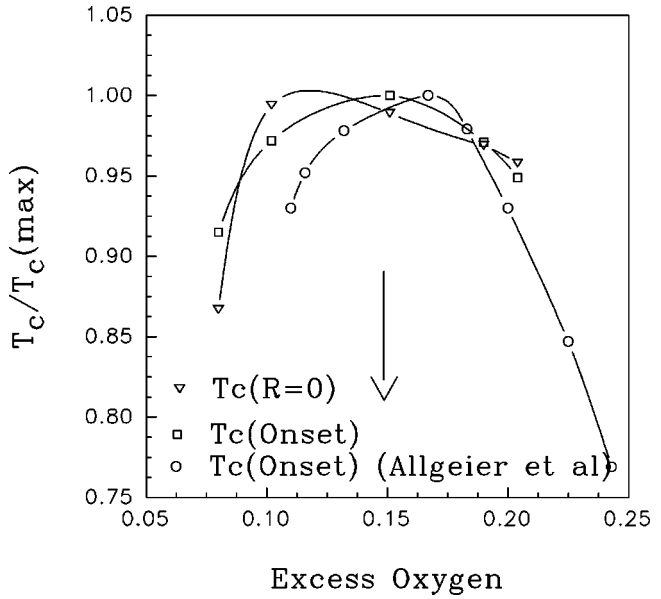


FIG. 8. $T_c/T_c$(max) as a function of excess oxygen content. The arrow points to the oxygen content for highest $T_c$(onset).

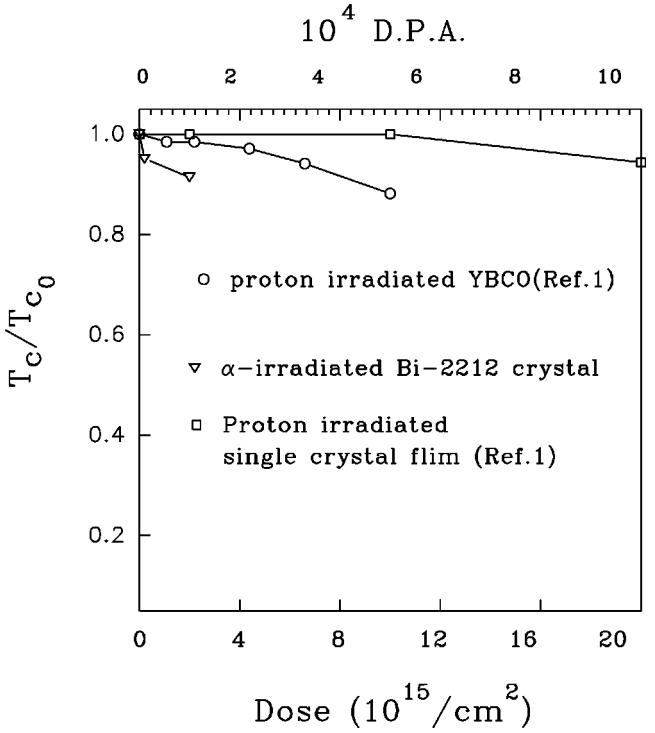


FIG. 9. $T_c/T_{c0}$ as a function of dose.

a decrease in the carrier concentration caused by the knock-out of oxygen by $\alpha$ particles. Linker *et al.*[9] also observed a decrease in $T_c$ for Bi-2212 film in the underdoped region and concluded that the defect structures connected to the $T_c$ depressions are mainly oxygen displacements.

The qualitative difference between changes in $T_c$ of polycrystalline and single-crystalline samples of Bi-2212 on particle irradiation (both proton and $\alpha$ particles) can thus be understood from the difference in the levels of doping in the unirradiated state; the single crystal is underdoped and polycrystals are overdoped with respect to oxygen. Particle irradiation causes knock-out of oxygen as well as an increase in transition width ($\Delta T_c$) for the reasons mentioned earlier. $T_c(R=0)$ changes due to irradiation are manifestations of both these effects.

If the superconducting pair wave function is written as $\Psi=\delta e^{i\kappa}$, where $\delta$ is the pair amplitude and $\kappa$ is the phase, then there are two ways to destroy superconductivity, either by reducing $\delta$, or by destroying the coherence of $\kappa$. In the case of A-15 superconductors irradiated with light charged particles like $\alpha$, there is a steady decrease in $T_c$ with the dose of irradiation until there is a saturation where the electronic mean free path is reduced to the level of interatomic spacing. Reduction in $T_c$ results from the lowering of electronic density of states due to increased electron defect scattering, i.e., amplitude reduction.[15] On the other hand, the behavior of high-$T_c$ superconductors is reminiscent of the destruction of phase coherence. Continuous broadening of the transition width with dose brings forth this fact.[16]

In Fig. 9, we have plotted $T_c(R=0)$ normalized with respect to $T_{c0}$ [where $T_{c0}$ is $T_c(R=0)$ for the unirradiated one] against fluence ($\Phi$) for our 40-MeV $\alpha$-irradiated Bi-2212 single crystal and proton irradiated YBCO films of Meyer[1] for comparison. A decrease in $T_c$ is fairly linear with dose. $dT_c/d\Phi$ comes out to be $2.77\times10^{-15}$ K/particle in the case

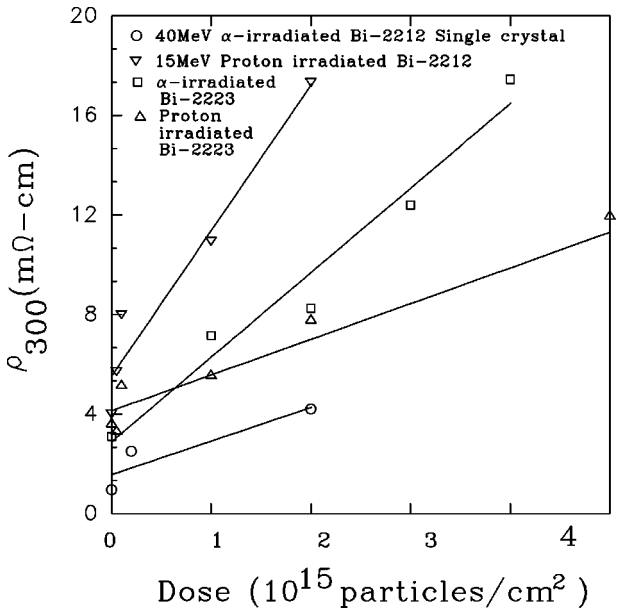


FIG. 10. Room-temperature resistivity ($r$) of irradiated samples as a function of dose.

of Bi-2212 single crystals, quite large as compared to that in single-crystalline YBCO film.[1] A decrease in $T_c$ in both cases is due to irradiation-induced knock-out of oxygen. $T_c$ depression by irradiation in the case of Bi-2212 single crystals is more than for YBCO films also when normalized with respect to d.p.a. Bi-2212 is more sensitive to particle irradiation than YBCO because of more defect stucture present.

The metallic behavior of resistivity is retained for all doses in proton irradiation and less than $1\times10^{16}/\mathrm{cm}^2$ in the case of $\alpha$ irradiation. We have plotted room-temperature resistivity ($\rho_{300}$) versus dose for 40-MeV $\alpha$ and 15-MeV proton irradiated Bi-2212 and Bi-2223 in Fig. 10. In the case of YBCO films irradiated with charged particles, the resistivity was increasing exponentially with fluence following the relation $\rho\cong\rho^0\exp(F_D\Phi/A)$,[17] where $\rho^0$ is the resistivity of the unirradiated sample, $F_D$ is the deposited energy, $\Phi$ is the dose, and $A$ is a constant with dimension of energy density. In our case, for all irradiated Bi-2212 and Bi-2223 samples, first-order linear fits in $\rho$ versus $\Phi$ are better than that for $\ln(\rho)$ versus $\Phi$. $\chi^2$ values for various fits are listed in Table IV. Contribution to a larger increase in $\rho$ with irradiation in the case of the polycrystal comes primarily from the grain boundaries where the point defect density is larger.

In comparison with Bi-2212, the rate of change in resistivity of Bi-2223 is less as evident from the respective slopes $d\rho/d\Phi$, $5.8\times10^{-15}$ m$\Omega$ cm/particle and $1.6\times10^{-15}$ m$\Omega$ cm/particle for proton irradiation, even though the d.p.a.'s in both cases are fairly close. The outdiffusion of oxygen in the grain boundary causing increase in resistivity is more dominant in irradiated polycrystalline Bi-2212 than in polycrystalline Bi-2223.

The marginal increase of $T_c$ and decrease of $\rho_{300}$ at the dose of $5\times10^{13}/\mathrm{cm}^2$ for Bi-2223 are indicative of annealing of defects at low dose. A similar decrease in resistivity was also noticed earlier in thin films of YBCO irradiated with a low dose of heavy ions ($10^{11}/\mathrm{cm}^2$) such as boron, arsenic, etc.,[17] and can be explained by the ordering brought about by the mobility of defects. At a low dose of irradiation, mobile defects were seen to increase the long-range order in partly ordered metallic alloys[18] and bring ordered structure in orthorhombic YBCO.[17] At higher fluences, radiation-induced disordering becomes dominant and hence, resistivity increases.

Variations of $d\rho/dT$ with dose for 40-MeV $\alpha$-irradiated Bi-2212 single crystals and Bi-2223 polycrystals and 15-MeV proton irradiated Bi-2212 and Bi-2223 are demonstrated in Figs. 11(a) and 11(b). Figure 11(a) shows the plots for $\alpha$ irradiation and Fig. 11(b) for proton irradiation. The dose in case of proton irradiation is given in log scale to cover a wide range, $5\times10^{13}$ to $5\times10^{15}/\mathrm{cm}^2$. $d\rho/dT$ of samples generally increased with the dose of irradiation. The increase of $d\rho/dT$ may be an indication of a decrease of $(n/m^*)$ with dose, where $n$ is the carrier concentration and $m^*$ is its effective mass.[19] In Bi-2212 system, the knock-out of excess oxygen may contribute to the reduction of hole carrier density. The increase of effective mass may occur due to radiation-induced disorder, and hence there is decrease of $(n/m^*)$ with irradiation which is dominant in the case of Bi-2223. In the case of Bi-2212, the slope of $d\rho/dT$ versus fluence comes out to be $3.6\times10^{-18}$ m$\Omega$ cm/K/particle and $1.7\times10^{-18}$ m$\Omega$ cm/K/particle for $\alpha$-irradiated single crystals and proton irradiated polycrystals, respectively.

### C. Nonmetallic resistivity at high doses

The resistivity changed from metallic to insulating behavior by $\alpha$ irradiation at a dose of $1\times10^{16}\alpha/\mathrm{cm}^2$ and higher for both Bi-2212 and Bi-2223 [Figs. 4(b) and 6(b), respectively]. The nonlinear behavior of resistivity is indicative of localization of charge carriers caused by irradiation-induced disorder. This was also observed by various groups in YBCO and Bi-Sr-Ca-Cu-O systems irradiated with neutrons at doses of $1\times10^{19}/\mathrm{cm}^2$ and higher.[20–22] The localization effect manifested in the case of neutrons at a dose higher than $7\times10^{18}/\mathrm{cm}^2$, is noticed in the case of 40-MeV $\alpha$ at a moderate dose of $1\times10^{16}/\mathrm{cm}^2$ for both Bi-2212 and Bi-2223. This is because of much higher energy deposited (by an order of 3 more than that of neutrons) in the case of 40-MeV $\alpha$-particles. The strong disorder induced in these systems at doses of $1\times10^{16}\alpha/\mathrm{cm}^2$ is revelant from the d.p.a. (1

TABLE IV. $\chi^2$ values for various fittings of resistivity versus dose.

| Sample | $\chi^2$ (exponential) | $\chi^2$ (linear) |
|---|---|---|
| Bi-2212 single crystal ($\alpha$ irradiated) | 0.1653 | $4.95\times10^{-2}$ |
| Bi-2212 polycrystal (proton irradiated) | 0.0850 | $2.28\times10^{-2}$ |
| Bi-2223 polycrystal ($\alpha$ irradiated) | 0.0300 | $1.80\times10^{-2}$ |
| Bi-2223 Polycrystal (proton irradiated) | 0.0600 | $3.66\times10^{-2}$ |

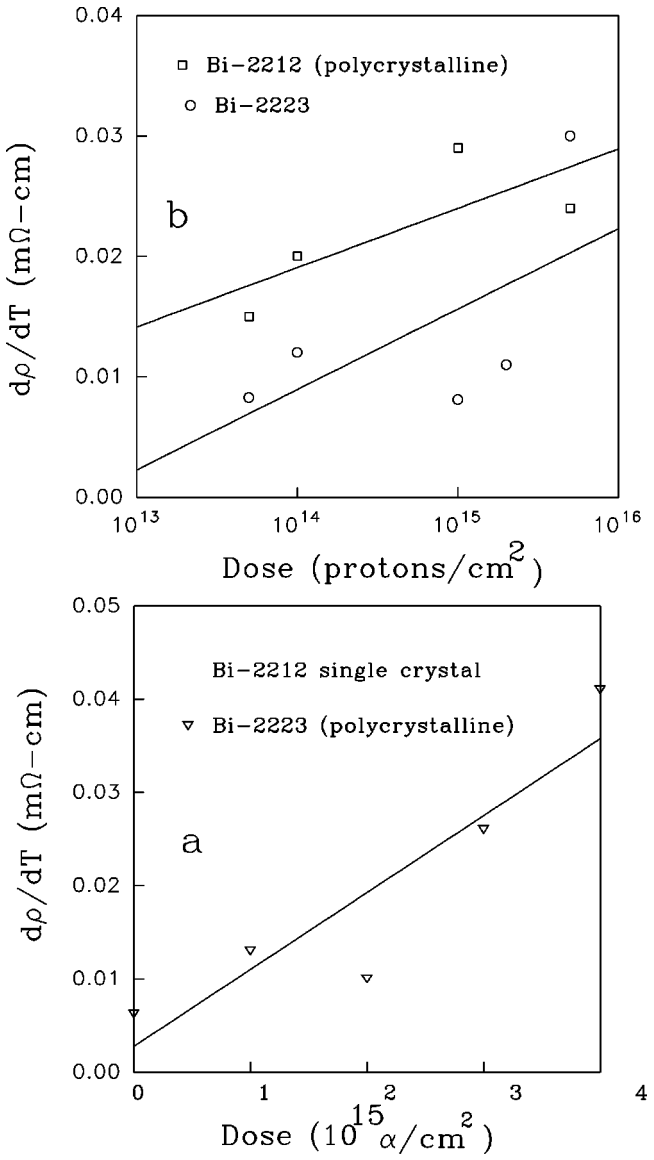


FIG. 11. Variation of $d\rho/dT$ with dose. (a) $\alpha$-irradiated Bi-2212 single crystals and polycrystalline Bi-2223. (b) Proton irradiated polycrystalline Bi-2212 and Bi-2223.

$\times 10^{-3}$), which is comparable to the neutrons at a dose of $1\times10^{19}$/cm$^2$. In Y-Ba-Cu-O, activated conduction was dominant in the nonmetallic region as evident from fairly linear behavior in the plot of the logarithm of resistance ($\ln R$) versus inverse of temperature ($1/T$).[20] In our case, ln ($\rho$) versus $1/T$ is not linear and we tried to analyze the nonlinear behavior of resistivity in the framework of variable range hopping (VRH). Normally, the resistivity in the insulating region is given by $\rho=\rho_0\exp[(T_0/T)^{1/(d+1)}]$, where the hopping conduction of carriers occurs in $d$-dimension.[23] Here, $T_0$ and $\rho_0$ are constants. Thus, for two-dimensional VRH, $\rho=\rho_0\exp[(T_0/T)^{1/3}]$, and for three-dimensional VRH, $\rho=\rho_0\exp[(T_0/T)^{1/4}]$.

In our case, the best fit was obtained in the case of the $\ln\rho$ vs $(T)^{-1/4}$ plot in the temperature range 256–115 K for Bi-2212 and 190–120 K for Bi-2223 (Fig. 12). Thus, the conduction in the nonmetallic region proceeds through three-dimensional (3D) VRH. A similar metal-to-insulator transition was observed in $Bi_2Sr_2Ca_{1-x}Y_xCu_2O_{8+x}$ at $x$

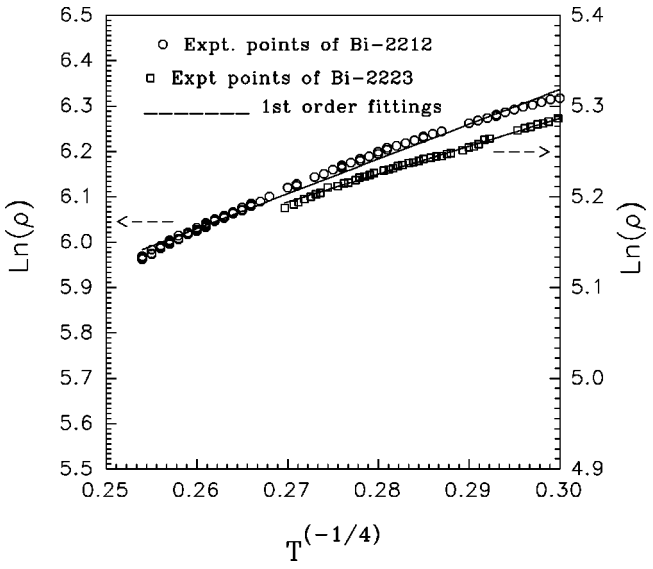


FIG. 12. Plot of 3D VRH fitting in nonmetallic part of resistivity.

$\geqslant 0.5$.[24,25] Substituting Y(III) in the Ca(II) site causes a lowering of carrier concentration. From the general phase diagram for these systems, it is now evident that they are Mott-Hubbard insulators at very low carrier concentration and become superconducting as the carrier concentration is increased to a certain extent and the normal-state behavior changes from insulator to metallic.[26–29] For the carrier concentration corresponding to the crossover region from metal to insulator, the conduction is generally seen to occur through 3D VRH.[30]

The reasons for transition from metal to insulator behavior of the irradiated sample at the highest dose may be twofold: (1) lowering of carrier concentration due to the knock-out of oxygen, (2) generation of localization caused by irradiation-induced disorder.[31] There is a difference between the irradiation-induced localizations in Bi-2212 and Bi-2223. In $\alpha$-irradiated Bi-2223, the change of carrier concentration due to change in oxygen content is not significant, which is dominant in $\alpha$-irradiated Bi-2212 as evident from iodometry. Rather localization caused by the radiation-induced disorder plays a major part in the case of Bi-2223.

We have estimated the localization length denoted as $\boldsymbol{\alpha}^{-1}$. For 3D VRH, $\boldsymbol{\alpha}^{-1}$ is derived from $T_0$ using the following expression: $T_0=(16\boldsymbol{\alpha}^3)/[k_BN(E_F)]$; $N(E_F)$ is the density of states at the Fermi level and $k_B$ is Boltzmann's constant. For Bi-2212, the values of $N(E_F)$ obtained from specific-heat data range from 1.25 to $5.62\times10^{-2}$ states/eV/Å$^3$ (for three dimensions).[32,33] We have taken the value $\sim$1.8 states/eV/Å$^3$.[30] The localization length ($\boldsymbol{\alpha}^{-1}$) is $\sim$10.7 Å. This value of $\boldsymbol{\alpha}^{-1}$ is quite low compared to that (60–80 Å) in the case of $Bi_2Sr_2Ca_{1-x}Y_xCu_2O_{8+x}$ in the 3D-VRH regime at the crossover of the metal-to-insulator transition (for $x=0.55$).[30] Our value is comparable to that for $x=0.6$. In the case of Bi-2223, the localization length ($\boldsymbol{\alpha^{-1}}$) is 10.6 Å, around five times the Cu-O bond length in $CuO_2$ plane.

## IV. MECHANISM OF OXYGEN KNOCK-OUT

The Cu-O bond in the $CuO_2$ sheet is the strongest bond and it controls the lattice constants.[34] The other layers in the

crystal structure are constrained to match the $CuO_2$ sheet and thus internal stress is generated within the crystal structure. The lattice stability in these cuprates is governed by a tolerance factor defined as[35]

$$t=\frac{A-O}{\sqrt{2}(B-O)}. \quad (1)$$

In Bi-2212, A-O and B-O are bond lengths of Bi-O in the rocksalt block and Cu-O in the perovskite block, respectively. In perovskites, for stable structure, the $t$ value should be as $0.8<t<0.9$.[35] If the bond lengths are taken to be the sum of the ionic radii of the respective ions, then with $r_{(Bi^{3+})}=0.93$ Å, $r_{(O^{2-})}=1.4$ Å, $r_{(Cu^{2+})}=0.72$ Å, $t$ comes out to be 0.78 in Bi-2212, and is less than the value needed for structural stability and an internal strain is developed. Since the Cu-O bond is rigid, the strain due to lattice mismatch can be relieved by the increase of the *A-O* bond length, which can be attained either by substitution of $Bi^{3+}$ by larger ions or by accommodating excess oxygen in the Bi-O layer. In undoped Bi-2212, the latter process occurs, whereby the Bi-O bond distance increases to 2.6 Å and the tolerance factor comes within proper range. This excess oxygen resides in the Bi-O layer because of more repulsion between the lone pair of electrons in $Bi^{3+}$ ions and oxygen along the *c*-axis.[34] The extra oxygen atoms form rows along the *a*-axis causing incommensurate modulation.[36] They are not valence bound. The binding energy of these extra oxygen atoms is very low ($\approx 0.073$ eV),[37] and hence they are vulnerable to be knocked out by energetic $\alpha$ particles and protons depending on the amount of energy deposited by the projectile.

The decrease in oxygen content (or the knock-out of oxygen) from the Bi-2212 sample can be understood to occur through the following steps: (1) Appreciable oxygen vacancies are created by charged particle irradiation-induced displacement at a dose $>1\times10^{15}$ particles/cm$^2$. (2) These displaced oxygen atoms occupy pores which are energetically favorable to them. (3) These ''free'' or labile oxygen molecules diffuse from pores to the outside (of the sample), which is in vacuum during irradiation.[37] This is the driving force for migration which is controlled by diffusion. The rate of oxygen atoms/molecules diffusing out is proportional to the atoms/molecules of oxygen present in pores. At room temperature, there is no reabsorption of oxygen by Bi-2212 and hence a net decrease in oxygen content occurs.

We have calculated with the help of the modified version (TRIM-95) of the simulation program TRIM developed by Biersack and Haggmark,[5] the number of vacancies created by displacement of loosely bound oxygen due to charged particle irradiation.[37] We have taken the binding energy of this loosely bound oxygen as 0.073 eV, supported by the experimentally observed $\Delta H$ value for liberation of loosely bound oxygen from the compound as obtained from thermogravimetric analysis (TGA) and differential thermal analysis (DTA).[38] The detailed calculations are presented elsewhere.[37] Values of the excess oxygen obtained from TRIM-95 calculations for Bi-2212 irradiated with 20-MeV $\alpha$, 40-MeV $\alpha$, and 15-MeV protons at various doses are presented in Table V. The data for 40-MeV $\alpha$ can be compared with the experimental values obtained by iodometry given in Table II. It is seen that these two data are in close agreement except for the highest dose. Thus, it establishes the mechanism of knock-out of oxygen by the charged particle irradiation followed by the diffusion from pores.

TABLE V. Excess oxygen values calculated from TRIM and diffusion.

| Dose (per cm$^2$) | 40-MeV $\alpha$ | 20-MeV $\alpha$ | 15-MeV proton |
|---|---|---|---|
| $2\times10^{15}$ | 0.1854 | 0.1914 | 0.1982 |
| $4\times10^{15}$ | 0.1480 | 0.1648 | 0.1861 |
| $6\times10^{15}$ | 0.1034 | 0.1335 | 0.1718 |
| $8\times10^{15}$ | 0.0553 | 0.0990 | 0.1564 |

The oxygen vacancies are created mostly in the bulk as little energy is lost at the surface and that through ionization. As the projectile particle loses energy with depth, the nonionizing energy loss dominates and displacement and the knock-out of oxygen become dominant. The damage profile in terms of oxygen vacancies in Bi-2212 with depth due to irradiation from both sides of the sample for proton irradiated Bi-2212 as a representative case has been shown in Fig. 13. In the case of proton irradiation, the damage distribution and hence, $T_c$, distribution are fairly uniform. This is the manifestation of irradiation from both sides of the samples. The minor local variations in $T_c$ due to oxygen contents cannot be probed as our resistivity measurements are global bulk ones. This variation occurs for all doses and would not affect the trend of data presentation in Fig. 8 which depicts the variation of $T_c$ normalized with respect to $T_c$(max) versus oxygen content varying with irradiation dose.

In Bi-2223 synthesized by partially doping Pb in the Bi site, the tensile stress in the Bi-O layer is relieved by substitution of larger $Pb^{2+}$ ions (1.2 Å) in the $Bi^{3+}$ (0.93 Å) site. So, Pb doped Bi-2223 does not accommodate excess oxygen significantly. Pb(II) substituting Bi(III) provides holes to $CuO_2$ layer, thereby relieving its compressive stress. Hence there is no loosely bound oxygen to be knocked out. In Bi-

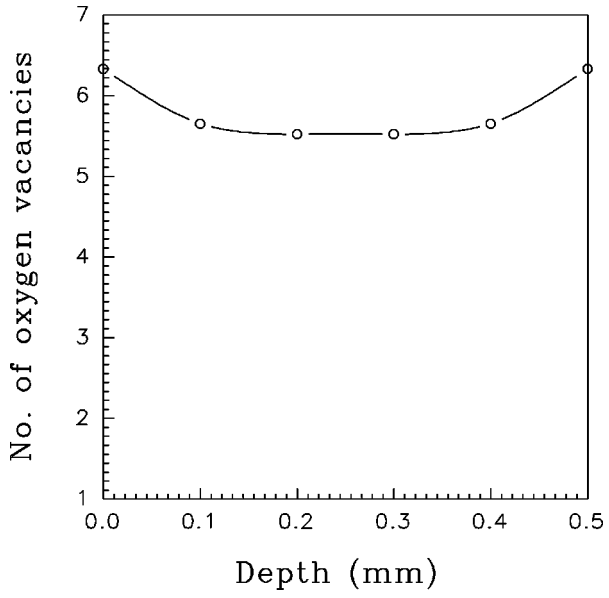


FIG. 13. Damage profile of proton in Bi-2212.

2223, because of the absence of loosely bound oxygen, only strong lattice bound oxygen comes into the picture for being knocked out. TRIM-95 calculations show the number of oxygen atoms displaced $\approx 5$/ion in case of Bi-2223, whereas the same in case of Bi-2212 containing loosely bound oxygen is around 110/ion.[37] This gives rise to the difference in Bi-2212 and Bi-2223 with respect to oxygen knock-out.

## V. CONCLUSION

We have carried out 40-MeV $\alpha$-particle and 15-MeV proton irradiations on $Bi_2Sr_2CaCu_2O_{8+x}$ (Bi-2212) and $Bi_{1.84}Pb_{0.34}Sr_{1.91}Ca_{2.03}Cu_{3.06}O_{10+x}$ (Bi-2223) at various doses up to $1\times10^{16}$ particles/cm$^2$. We have employed both single-crystal and polycrystalline samples in the case of Bi-2212 and polycrystalline samples in the case of Bi-2223 systems for irradiation. There was little evidence of structural breakdown or phase change. In Bi-2212, there were distinct evidences of the knock-out of oxygen caused by particle irradiation. In case of the bulk polycrystalline samples, this was confirmed by iodometric estimation of oxygen. The manifestation of this irradiation-induced knock-out of oxygen and hence decrease of the carrier concentration was the increase of $T_c$ in Bi-2212 overdoped with oxygen. On the other hand, in Bi-2223, the knock-out of oxygen is not significant. This is reflected in the changes of their physical properties such as $T_c$, resistivity, etc., by irradiation. Theoretical estimates have been done for the amounts of oxygen knocked out in irradiated Bi-2212 at various doses using Monte Carlo program TRIM-95 and there have been close agreements with the experimental values obtained by iodometry. At a high dose of $1\times10^{16}\alpha$/cm$^2$, there is a change to nonmetallic behavior in resistivity with 3D VRH conductivity in both Bi-2212 and Bi-2223. The change in behavior of resistivity in Bi-2212 was due to the decrease in oxygen or, hole carrier concentration so as to cause a transition from metallic to insulator region. We have calculated the localization length and it comes to be low, around 3–5 times the Cu-O bond length in the $CuO_2$ layer. In contrast, the metal-insulator transition brought about by $\alpha$ irradiation in Bi-2223 is not due to the lowering of hole carrier concentration, but due to some kind of localization caused by the irradiation-induced disorder. Here also, the localization length is quite low.

## ACKNOWLEDGMENTS

The authors are grateful to Dr. B. Sinha, Director, V. E. C. Centre, Calcutta for his constant encouragement and help. One of the authors (A.K.G.) acknowledges financial help from University Grants Commission (U.G.C.). Authors also acknowledge their gratitude towards Humboldt Foundation for the Leyboldt 10-300 cryogenerator.

[1] O. Meyer, in *Studies of High Temperature Superconductors*, edited by A. V. Narlikar (Nova Science Publishers, New York, 1989), Vol. 1, p. 139 and the references therein.

[2] L. F. Mattheiss and R. L. Testardi, Phys. Rev. B **20**, 2196 (1979); Phys. Rev. Lett. **41**, 1612 (1978).

[3] N. Nucker, J. Fink, J. C. Fuggle, P. J. Durham, and W. M. Temmermann, Phys. Rev. B **37**, 5158 (1988).

[4] S. K. Bandyopadhyay, P. Barat, S. Kar, U. De, A. Poddar, P. Mandal, B. Ghosh, and C. K. Majumdar, Solid State Commun. **82**, 397 (1992).

[5] J. P. Biersack and L. G. Haggmark, Nucl. Instrum. Methods **174**, 257 (1980).

[6] N. Knauf, J. Harnischmacher, R. Muller, R. Borowski, B. Roden, and D. Wohlleben, Physica C **173**, 414 (1991).

[7] U. Endo, S. Koyama, and T. Kawai, Jpn. J. Appl. Phys., Part 2 **28**, L190 (1989).

[8] E. H. Appelman, L. R. Morss, A. M. Kini, U. Geiser, A. Umezawa, G. W. Crabtree, and K. D. Carlson, Inorg. Chem. **26**, 3237 (1987).

[9] G. Linker, J. Geerk, T. Kroener, O. Meyer, J. Remmel, R. Smithey, B. Strehlau, and X. X. Xi, Nucl. Instrum. Methods Phys. Res. B **59-60**, 1458 (1991).

[10] G. J. Clark, A. D. Marwick, F. K. Le Goves, R. B. Laibowitz, R. Koch, and P. B. Madakson, Nucl. Instrum. Methods Phys. Res. B **32**, 405 (1988).

[11] G. J. Clark, A. D. Marwick, R. M. Koch, and R. B. Laibowitz, Appl. Phys. Lett. **51**, 139 (1987).

[12] M. O. Ruault and M. Gasgnier, Mater. Sci. Eng. B **5**, 57 (1989).

[13] C. Allgeier and J. S. Schilling, Physica C **168**, 499 (1990).

[14] J. M. Tarascon, Y. LePage, P. Bardoux, B. G. Bagley, L. H. Greene, W. R. McKinnon, G. W. Hull, M. Giroud, and D. M. Hwang, Phys. Rev. B **37**, 9382 (1988).

[15] J. M. Poate, R. C. Dynes, and L. R. Testardi, Phys. Rev. Lett. **37**, 1308 (1976).

[16] A. E. White, K. T. Short, J. M. Poate, R. C. Dynes, P. M. Mankiewich, W. J. Skocpol, R. E. Howard, H. Anzlowar, K. W. Baldwin, A. F. J. Levi, J. R. Kwo, T. Hsieh, and M. Hong, Phys. Rev. B **37**, 3755 (1988).

[17] A. D. Marwick, G. J. Clark, D. S. Yee, R. B. Laibowitz, G. Coleman, and J. J. Como, Phys. Rev. B **39**, 9061 (1989).

[18] E. M. Schulson, J. Nucl. Mater. **83**, 239 (1979).

[19] T. Ito, K. Takenaka, and S. Uchida, Phys. Rev. Lett. **70**, 3995 (1993).

[20] G. C. Xiong, H. C. Li, G. Linker, and O. Meyer, Physica C **153-155**, 1447 (1988); Phys. Rev. B **38**, 240 (1988).

[21] B. A. Aleksashin, I. F. Berger, S. V. Verkhovskii, V. I. Voronin, B. N. Goshchitskii, S. A. Davydov, A. E. Karkin, V. L. Kozhevivnikov, A. V. Mirmelśhtein, K. N. Mikhalev, V. D. Parkhomenko, and S. M. Chesnitskii, Physica C **153-155**, 339 (1988).

[22] B. A. Aleksashin, V. P. Voronin, S. V. Verkhovskii, B. N. Goshchitskii, S. A. Davydov, Yu. I. Zhadnov, A. E. Karkin, V. L. Kozhevivnikov, A. V. Mirmelśhtein, K. N. Mikhalev, M. V. Sadovskii, V. V. Serikov, and S. M. Chesnitskii, Zh. Eksp. Teor. Fiz. **95**, 678 (1989) [Sov. Phys. JETP **68**, 382 (1989)].

[23] N. F. Mott, *Metal Insulator Transitions* (Taylor and Francis, London, 1974).

[24] T. Tamegai, K. Koga, K. Suzuki, M. Ichimara, F. Sakai, and Y. Iye, Jpn. J. Appl. Phys., Part 2 **28**, L112 (1989).

[25] R. Yoshizaki, Y. Saito, Y. Abe, and H. Ikeda, Physica C **152**, 408 (1988).

[26] J. B. Torrance, Y. Tokura, A. I. Nazzal, A. Bezinge, T. C. Huang,

and S. S. P. Parkin, Phys. Rev. Lett. **61**, 1127 (1988).
[27] Y. Shimakawa, Y. Kubo, T. Manako, and H. Igarashi, Phys. Rev. B **40**, 11 400 (1989).
[28] A. Matsuda, K. Kinoshita, T. Ishii, H. Shibata, T. Watanabe, and T. Yamada, Phys. Rev. B **38**, 2910 (1988).
[29] Z. Z. Wang, J. Clayhold, N. P. Ong, J. M. Tarascon, L. H. Greene, W. R. McKinnon, and G. W. Hull, Phys. Rev. B **36**, 7222 (1987).
[30] P. Mandal, A. Poddar, B. Ghosh, and P. Choudhury, Phys. Rev. B **43**, 13 102 (1991).
[31] P. W. Anderson, Phys. Rev. **109**, 1492 (1958).
[32] R. A. Fisher, S. Kim, S. E. Lacy, N. E. Phillips, D. E. Morris, A. G. Markelz, J. Y. T. Wei, and D. S. Ginley, Phys. Rev. B **38**, 11 942 (1988).
[33] N. Okazaki, T. Hasegawa, K. Kishio, K. Kitazawa, A. Kishi, Y. Ikeda, M. Takano, K. Oda, H. Kitaguchi, J. Takada, and Y. Miura, Phys. Rev. B **41** , 4296 (1990).
[34] H. Zhang and H. Sato, Physica C **214**, 265 (1993).
[35] F. S. Galasso, *Structure, Properties and Preparation of Perovskite-Type Compounds* (Pergamon, New York, 1969), p. 4.
[36] S. B. Samanta, P. K. Dutta, V. P. S. Awana, E. Gmelin, and A. V. Narlikar, Physica C **178**, 171 (1991).
[37] S. K. Bandyopadhyay, Pintu Sen, P. Barat, P. Mukherjee, S. K. Das, and B. Ghosh, Pramana, J. Phys. **47**, 309 (1996); S. K. Bandyopadhyay, A. K. Ghosh, P. Barat, Pintu Sen, A. N. Basu, and B. Ghosh, Phys. Status Solidi A **162**, 701 (1997).
[38] G. Moiseev, N. Vatolin, and J. Sestak, Thermochim. Acta **266**, 285 (1995); **217**, 309 (1993); **237**, 401 (1994).